



High Resolution Powder Diffractometer (HRPD) Design

Alan Hewat, Diffraction Group, ILL.

Objectives for an HRPD:

- Precise structures using Rietveld Refinement
- High resolution over the whole pattern
- High intensity for rapid experiments on small samples

These objectives are mutually incompatible

- Intensity decreases with resolution etc

The best compromises -> the most useful machine



HRPD Design Objectives

Objectives:

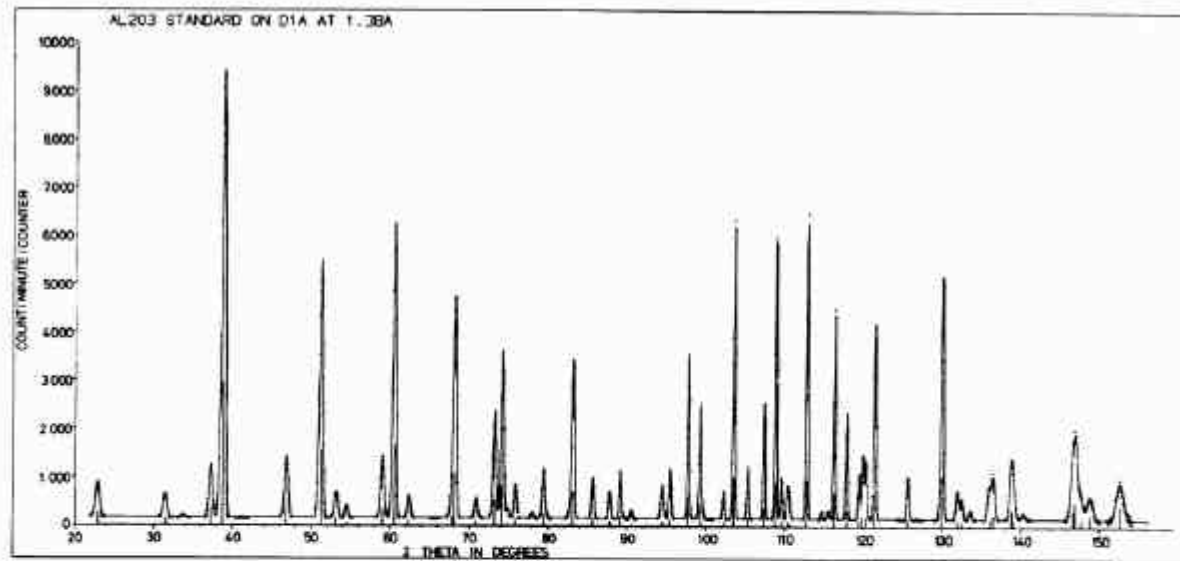
- High resolution

+

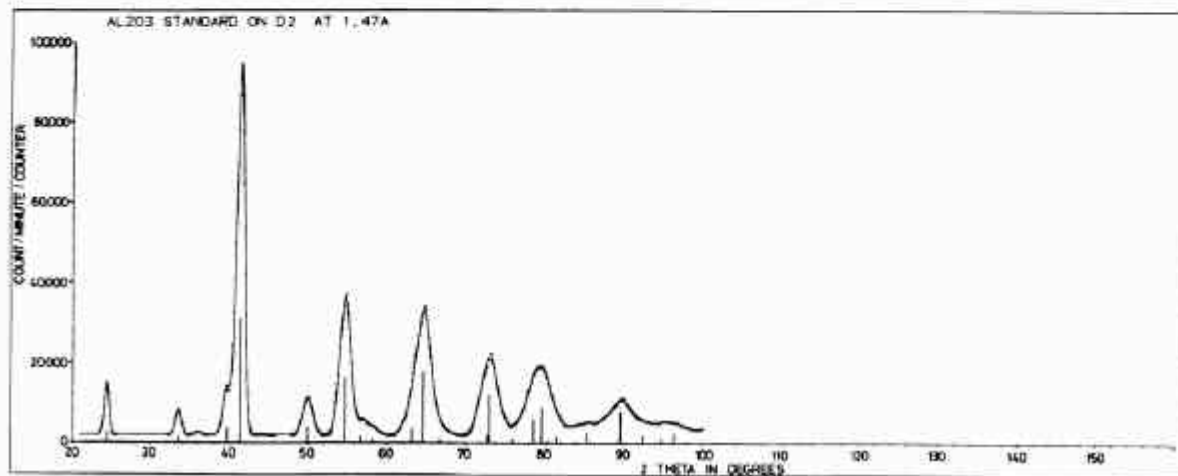
- High intensity

a) Good compromise

b) Bad compromise



(a)



(b)



High Resolution at High Angles

Bragg's law: $2d \cdot \sin \mathbf{q} / \mathbf{l} = p^{1/2}$ where: $p = h^2 + k^2 + l^2$

Differentiate: $2 \cdot \frac{d\mathbf{d}}{d\mathbf{q}} \cdot \cos \mathbf{q} / \mathbf{l} = p^{1/2} = 2d \cdot \sin \mathbf{q} / \mathbf{l}$

Resolution: $\frac{D\mathbf{d}}{d} = D\mathbf{q} \cdot \cot \mathbf{q}$ ($\cot \mathbf{q}$ small for \mathbf{q} large)

cf Neutrons

$$2\mathbf{q}_{\max} \sim 160^\circ$$

$$\cot \mathbf{q} \sim 0.176$$

$$D\mathbf{q} \sim 0.15^\circ \sim 3 \cdot 10^{-3} \text{ rad}$$

$$\frac{D\mathbf{d}}{d} \sim 5 \cdot 10^{-4}$$

X-ray synchrotron

$$2\mathbf{q}_{\max} \sim 80^\circ$$

$$\cot \mathbf{q} \sim 1.2$$

$$D\mathbf{q} \sim 0.03^\circ \sim 6 \cdot 10^{-4} \text{ rad}$$

$$\frac{D\mathbf{d}}{d} \sim 7 \cdot 10^{-4}$$

High Resolution at High Angles



Neutron d/d resolution
can compete with
Synchrotron resolution

But ! Neutron diffraction requires high angle scattering
(backscattering)



Resolution vs Intensity

Bragg's law: $2d \cdot \sin \mathbf{q} / \mathbf{l} = p^{1/2}$ where: $p = h^2 + k^2 + l^2$

Differentiate: $2 \cdot \frac{d\mathbf{l}}{d\mathbf{q}} \cdot \cos \mathbf{q} / \mathbf{l} = p^{1/2} = 2d \cdot \sin \mathbf{q} / \mathbf{l}$

Intensity: $\frac{d\mathbf{l}}{\mathbf{l}} = \frac{d\mathbf{q}_M}{\mathbf{q}_M} \cdot \cot \mathbf{q}_M$ cf $\frac{d\mathbf{d}}{d} = \frac{d\mathbf{q}}{\mathbf{q}} \cdot \cot \mathbf{q}$

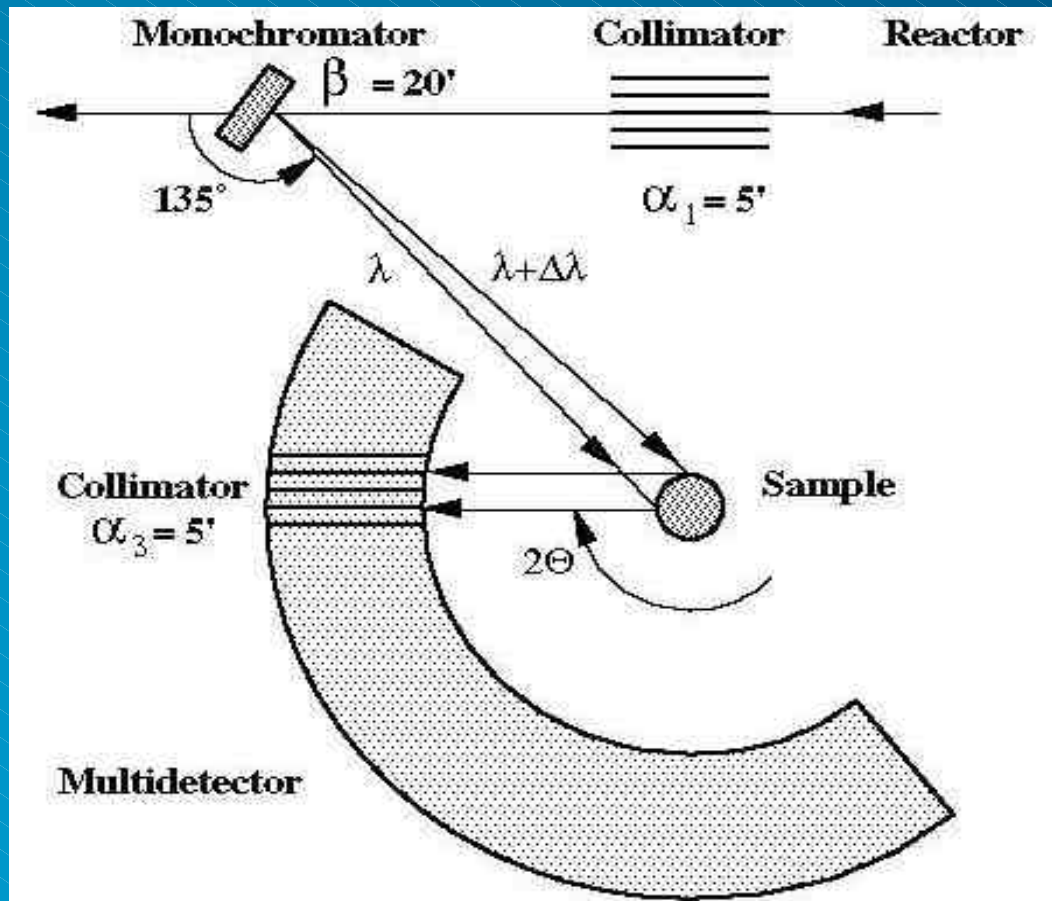
High resolution $\frac{d\mathbf{d}}{d}$ implies low intensity $\frac{d\mathbf{l}}{\mathbf{l}}$ unless $\frac{d\mathbf{q}_M}{\mathbf{q}_M}$ large

Need large monochromator mosaic $\frac{d\mathbf{q}_M}{\mathbf{q}_M} = \mathbf{b}$

Fortunately, resolution (focusing) does not depend on $\frac{d\mathbf{q}_M}{\mathbf{q}_M} = \mathbf{b}$



Powder Diffractometers are Simple



- A continuous neutron source
- Incident collimation
- A Monochromator
- The Sample & environment
- Scattering collimation
- A Detector



Resolution vs Scattering Angle $2\mathbf{q}$

If A = Full Width at Half Maximum (FWHM) of Bragg peak

Cagliotti formula: $A^2 = U \cdot \tan^2 \mathbf{q} + V \cdot \tan \mathbf{q} + W$

Where:

$$U = (2.5\mathbf{a}_1^2 + 2\mathbf{b}^2) \cdot \tan^{-2} \mathbf{q}_M$$

$$V = -(2\mathbf{a}_1^2 + 4\mathbf{b}^2) \cdot \tan^{-1} \mathbf{q}_M$$

$$W = 0.5\mathbf{a}_1^2 + 2\mathbf{b}^2 + \mathbf{a}_3^2$$

Where \mathbf{a}_1 , \mathbf{a}_2 , \mathbf{a}_3 are the beam divergences

\mathbf{b} is the monochromator mosaic

Differentiating, the minimum peak width occurs for:

$$\mathbf{q} = \mathbf{q}_M \quad \text{and} \quad A^2 \sim (\mathbf{a}_1^2 + \mathbf{a}_3^2)$$



Resolution vs Scattering Angle \mathbf{q}

Best resolution occurs when:

$$\mathbf{q} = \mathbf{q}_M \quad \text{and} \quad A^2 \sim (\mathbf{a}_1^2 + \mathbf{a}_3^2)$$

(focussing condition)

Best resolution at focus depends only on collimation $\mathbf{a}_1 \sim \mathbf{a}_3$

Best Intensity $\sim \mathbf{a}_1 \mathbf{a}_2 \mathbf{a}_3 \mathbf{b}$

Density of peaks \rightarrow Large monochromator angle ($> 90^\circ$)



Vertically Focusing Monochromator

Vertical focusing does not affect resolution (at 90° focussing)

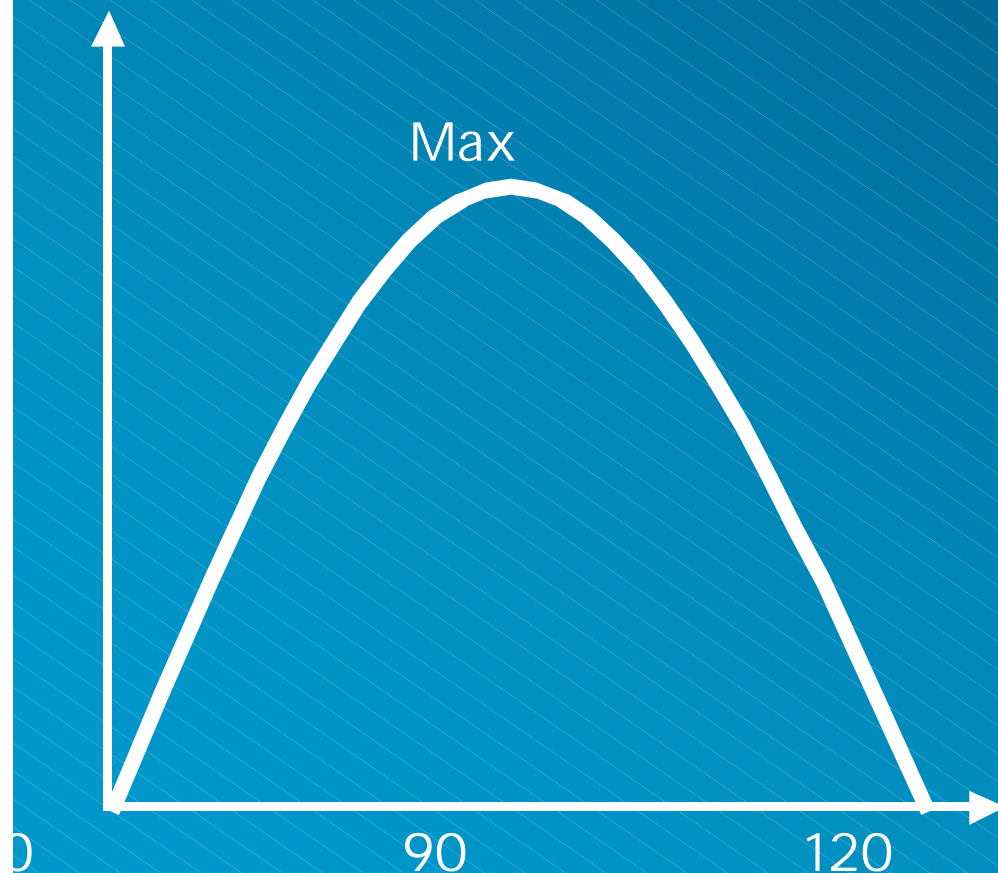
But how do we obtain good resolution at large d-spacings ?

Use long wavelengths λ to get large d-spacings at large angles



High Resolution at High Angles

Density of Peaks $\delta p / \delta \theta$



Match instrument to resolution required to resolve Bragg peaks.

Bragg's law: $2d \cdot \sin \mathbf{q} / \mathbf{l} = p^{1/2}$

where: $p = h^2 + k^2 + l^2$

Differentiate $d\mathbf{p} / d\mathbf{q}$

Density p : $d\mathbf{p} / d\mathbf{q} = (2d / \mathbf{l})^2 \cdot \sin 2\mathbf{q}$

Angle between peaks, put $d\mathbf{p} = 1$

$\mathbf{D}(2\mathbf{q}) = 2\mathbf{D}(\mathbf{q}) = 2(\mathbf{l} / 2d)^2 / \sin 2\mathbf{q}$



High Resolution at High Angles

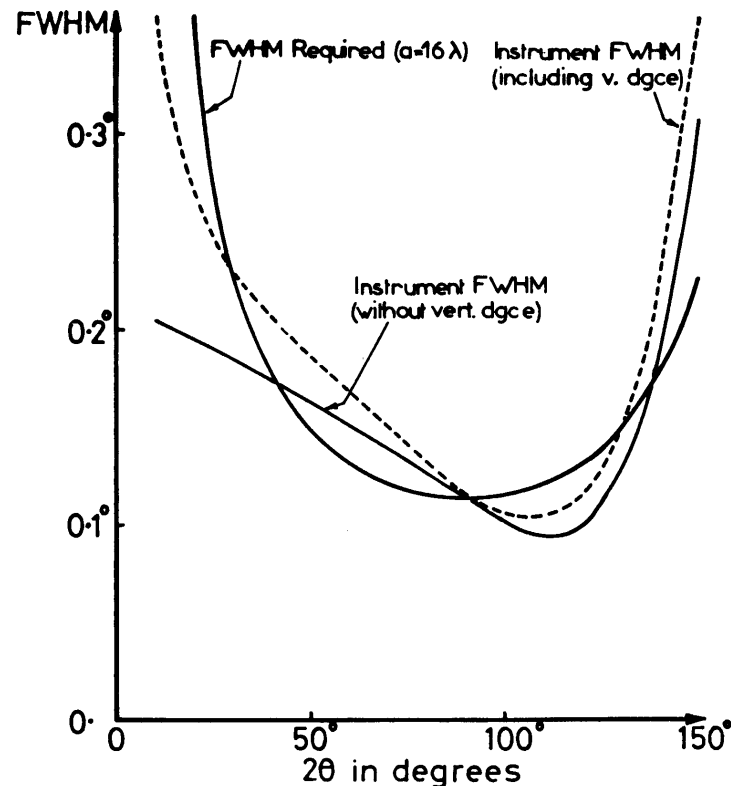


Fig. 1. Full width at half height for a high-resolution ($\alpha = 0.1^\circ/\sqrt{2}$) conventional powder diffractometer with $\alpha_1 = \alpha_3 = \alpha$, $\beta = 2\alpha$ and $\alpha_2 = 2\beta$. These collimators, α_i , and monochromator mosaic spread, β , have been chosen so that the diffractometer resolution (solid line) matches that required to resolve adjacent lines for an hypothetical cubic crystal of lattice dimension $a = 24 \text{ \AA}$ (points), with maximum line intensity.

Match instrument to resolution required to resolve Bragg peaks.

Bragg's law: $2d \cdot \sin \mathbf{q}/\mathbf{l} = p^{1/2}$

where: $p = h^2 + k^2 + l^2$

Differentiate $d\mathbf{p}/d\mathbf{q}$

Density p : $d\mathbf{p}/d\mathbf{q} = (2d/\mathbf{l})^2 \cdot \sin 2\mathbf{q}$

Angle between peaks, put $d\mathbf{p} = 1$

$D(2\mathbf{q}) = 2D(\mathbf{q}) = 2(\mathbf{l}/2d)^2 / \sin 2\mathbf{q}$

Focussing with equal monochromator & detector angles

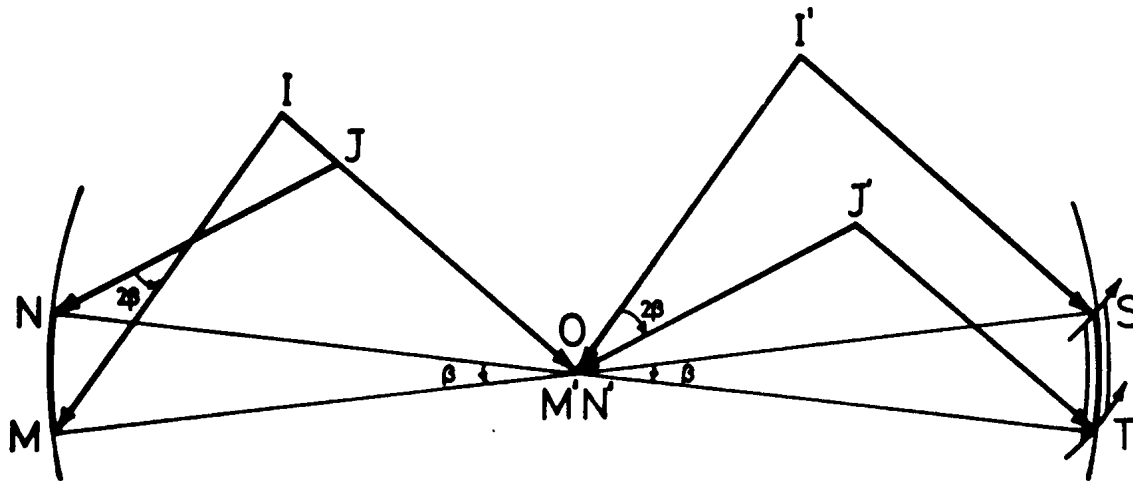


Fig. 2. Reciprocal space focussing for parallel geometry in which the collimators α_1 and α_3 are parallel, i.e. the counter collects $I'S$ and $J'T$ parallel to IO incident on the monochromator. Then the Ewald sphere ST , which is an image of the arc MN representing the monochromator mosaic spread β , cuts through the powder diffraction sphere at a tangent. The line shape is independent of β and α_2 , being simply the convolution of the triangular transmission functions for α_1 and $\alpha_3 = \alpha_1$.

Backscattering TOF focussing

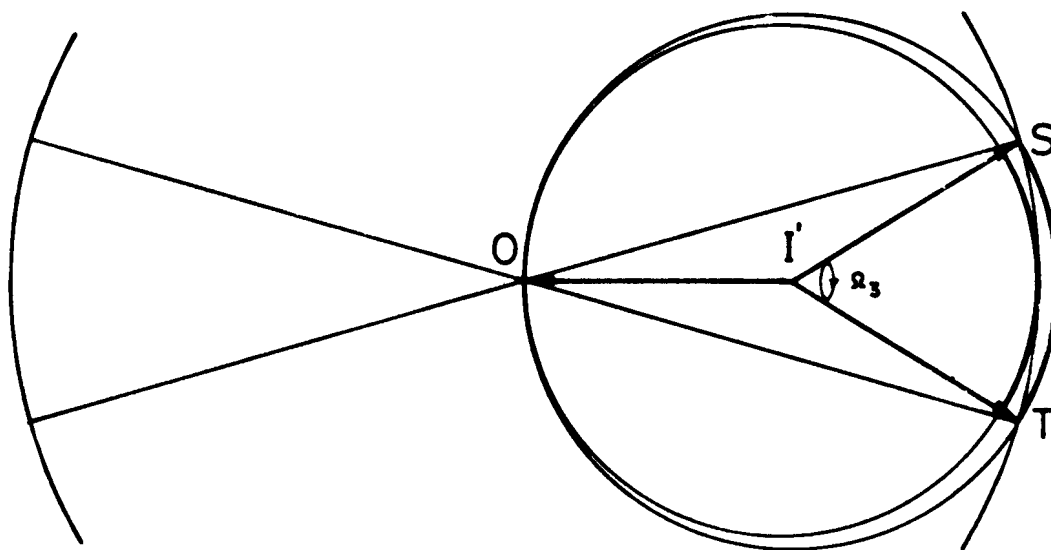


Fig. 3. Backscattering TOF geometry in reciprocal space. When the neutron wavelength is varied, the Ewald sphere ST cuts through the powder diffraction sphere at a tangent. Scattering occurs almost simultaneously for a large solid angle Ω_3 in the backscattering direction ($2\theta = 180^\circ$), c.f. fig. 2. The line width depends on the “collimation” Ω_1 and Ω_3 of the incident and scattered beams, and on the spread in the measurement of the neutron wavelength (velocity).



Required Resolution

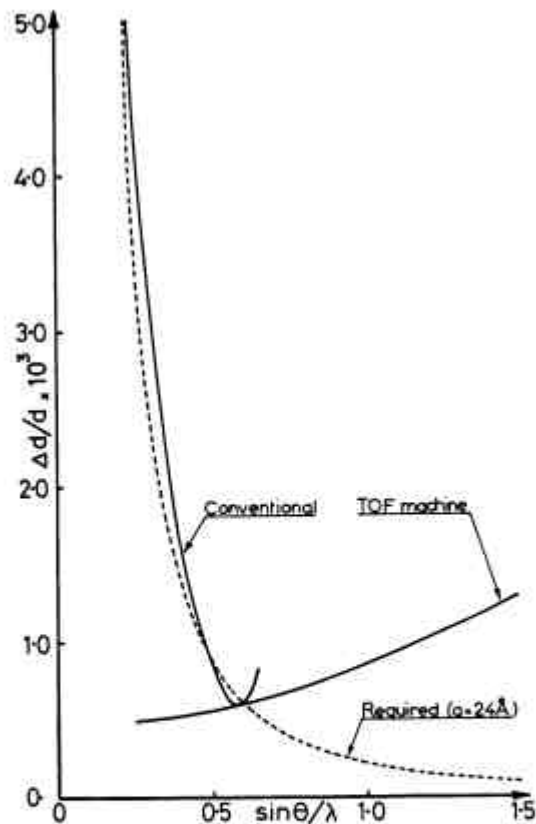


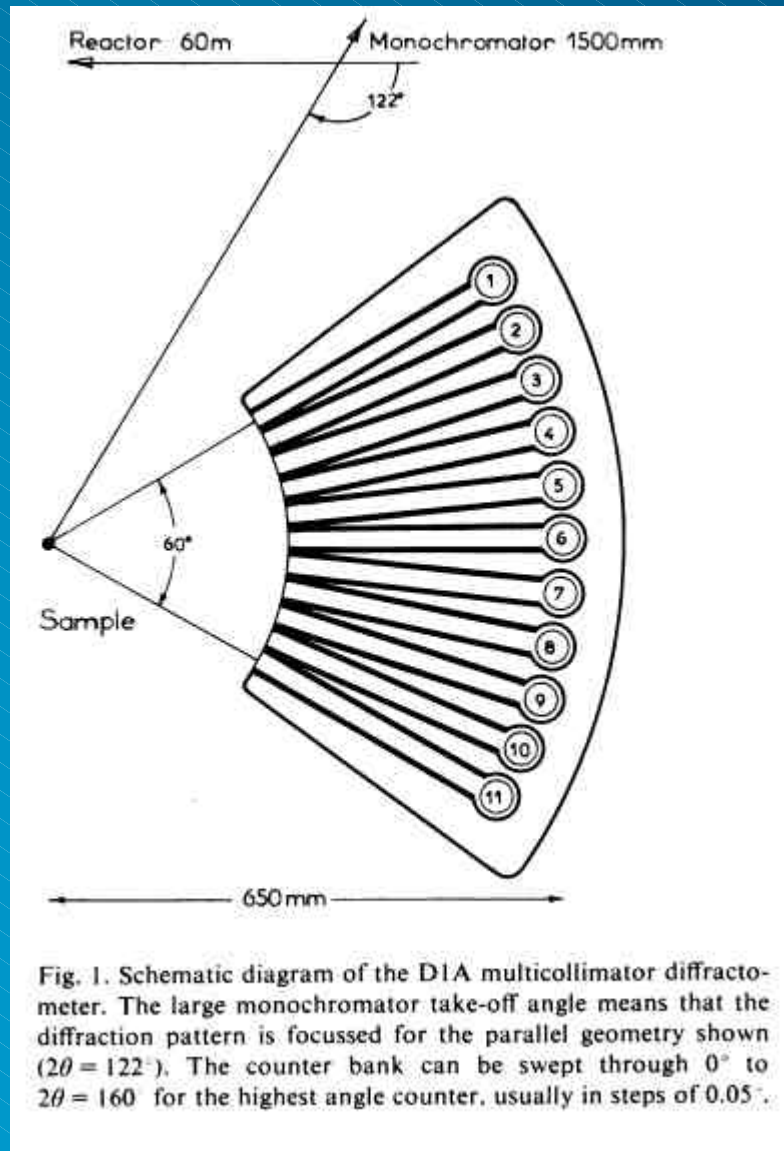
Fig. 4. Resolution functions for the conventional and back-scattering TOF powder diffractometers, compared to that required to resolve adjacent lines for a cubic crystal with $a = 24 \text{ \AA}$. The TOF machine has higher resolution for low ($\sin \theta/\lambda$), and lower resolution than required for high ($\sin \theta/\lambda$). The conventional machine can be designed to match the resolution required at low and medium ($\sin \theta/\lambda$), but the high ($\sin \theta/\lambda$) region cannot be reached, unless the wavelength is reduced, and then the resolution again falls below that required.

Conventional reactor HRPD matches resolution required to resolve adjacent peaks.

Time-of-Flight machine has best resolution at large d - a poor match.



D1A, high resolution multi-detector



Note:

- large monochromator angle
- large scattering angles
- large multi-detector bank

Very successful machine for Rietveld refinement.



Limited scattering volume

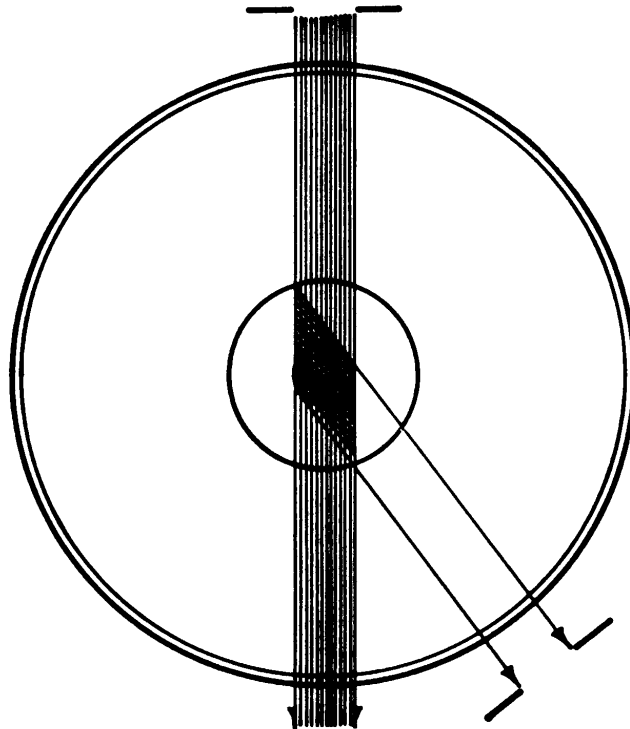


Fig. 5. The scattering volume seen by the position-sensitive detector and backscattering TOF machines (shaded) is larger than that seen by the conventional diffractometer (cross-hatched). This can be important if the sample is enclosed in a cryostat or furnace. On the other hand, with the backscattering machine one small window serves for both the incident and scattered beams.

The collimators define
small scattering volume

Eliminate scattering
from sample environment



High resolution from collimators

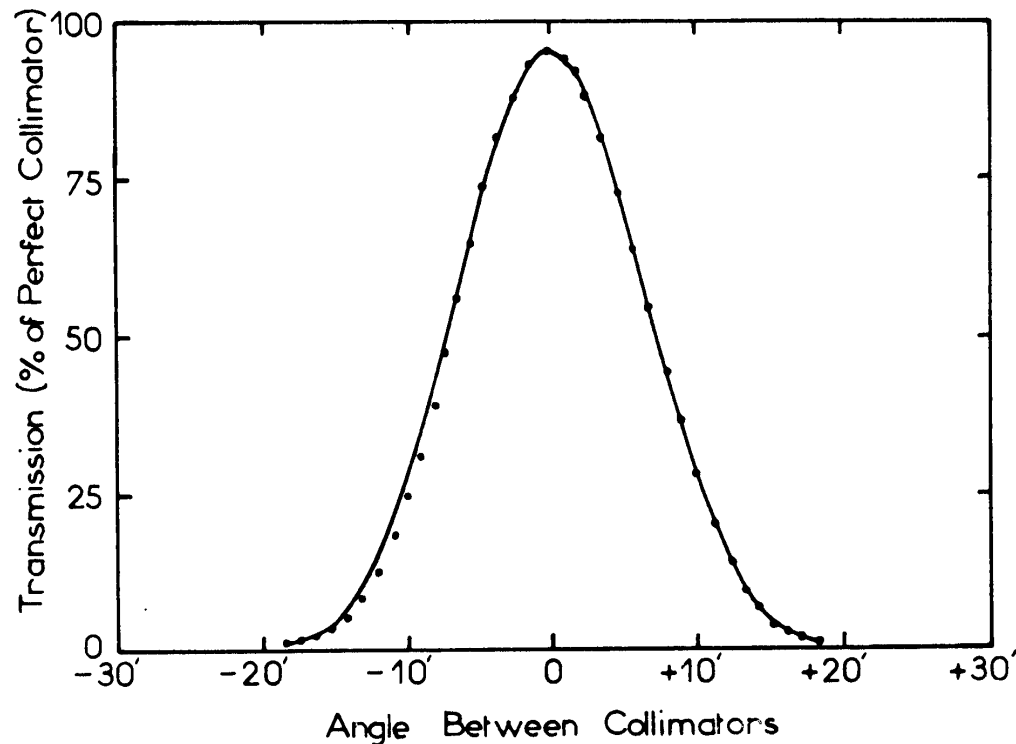


Fig. 2. Observed and calculated profiles for two 10' mylar collimators rocked against each other (from ref. 6). The horizontal axis gives the angle between the collimators and the vertical axis shows the transmission of the second collimator as a percentage of that expected for an "ideal" collimator.

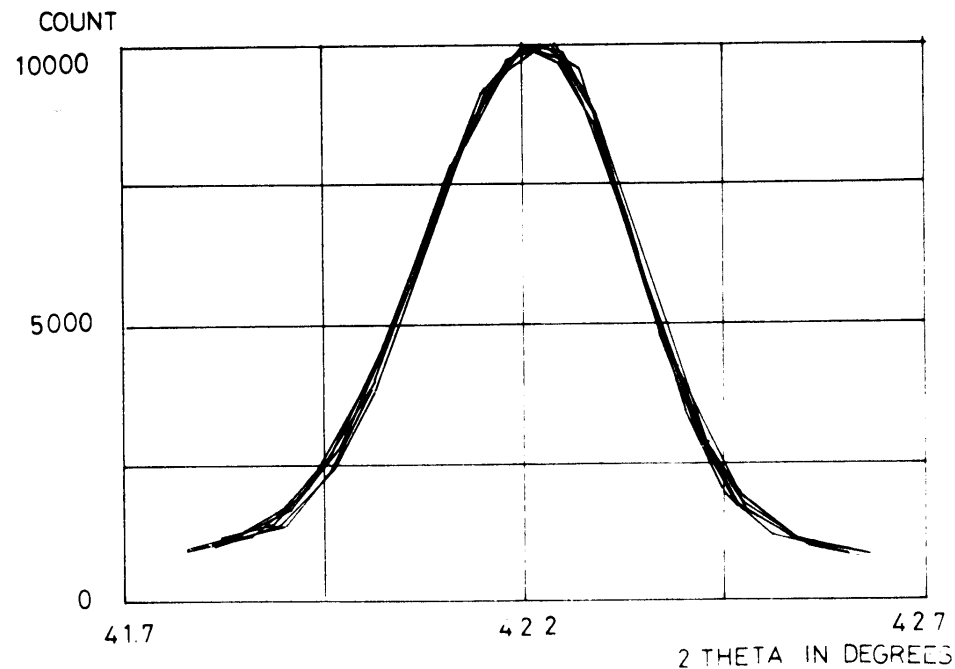
At focusing angle, the resolution depends only on the collimators

-

NOT on monochromator, wavelength spread etc...



Uniformity of Collimators



(b)

Fig. 3. (a) The $|311| \text{Al}_2\text{O}_3$ peak as seen by the first six collimator/counters. The errors shown here in collimator alignment ($\pm 0.02^\circ$) and counter efficiency ($\pm 4\%$) are corrected by interpolation and scaling. (b) As a result of these corrections, the separate profiles are now effectively identical, and can be added to produce a single composite profile for refinement. The whole process is of course automatic, being part of the data retrieval program. This program also compares each of the profiles to pick up any systematic errors (e.g. time dependent noise).

The collimators must be identical because we must add the separate patterns together...

...after correcting for relative displacement and efficiency...



HRPD Design Objectives

Objectives:

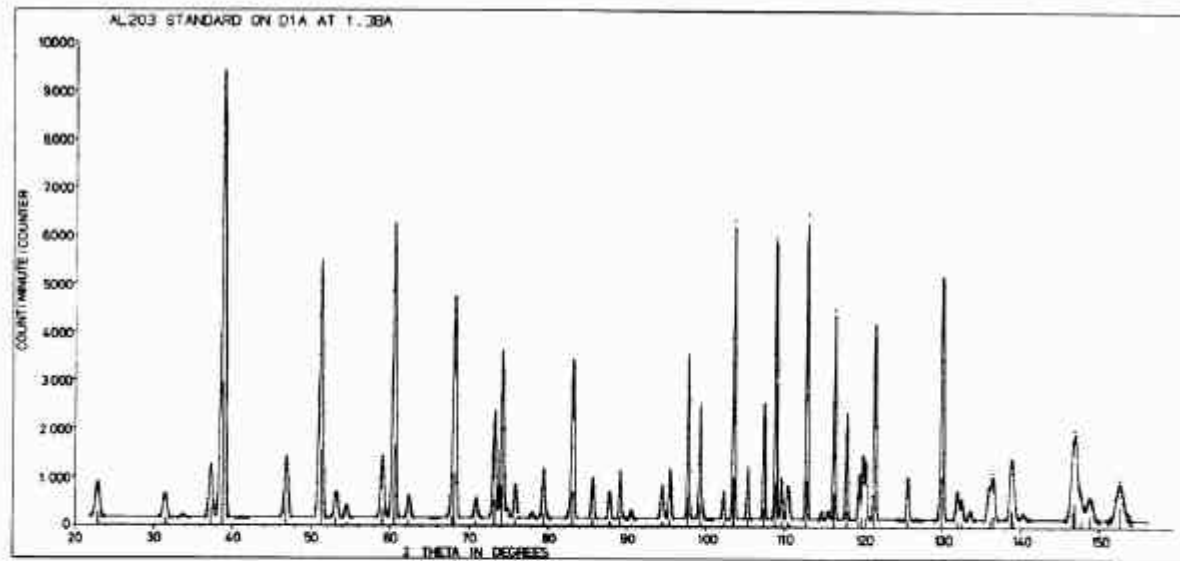
- High resolution

+

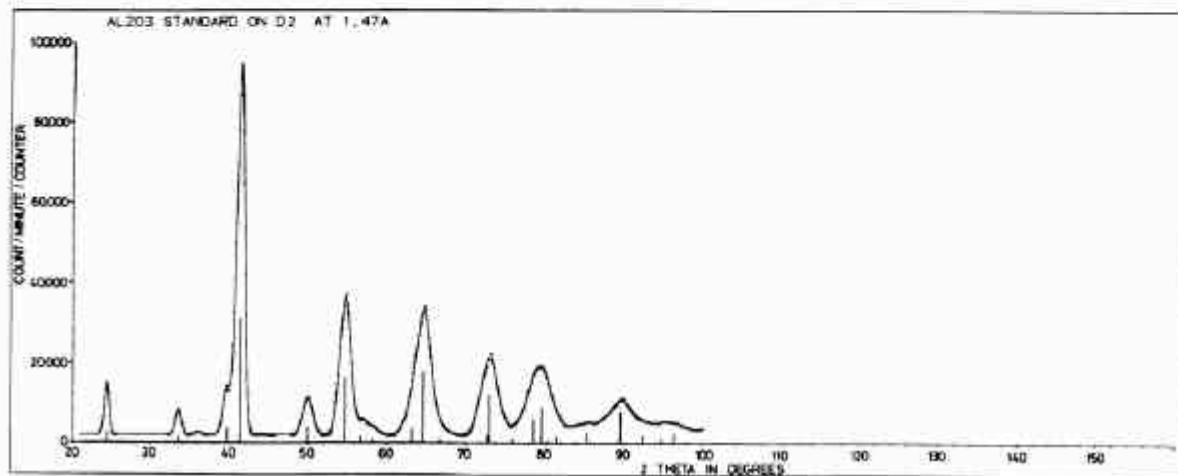
- High intensity

a) Good compromise

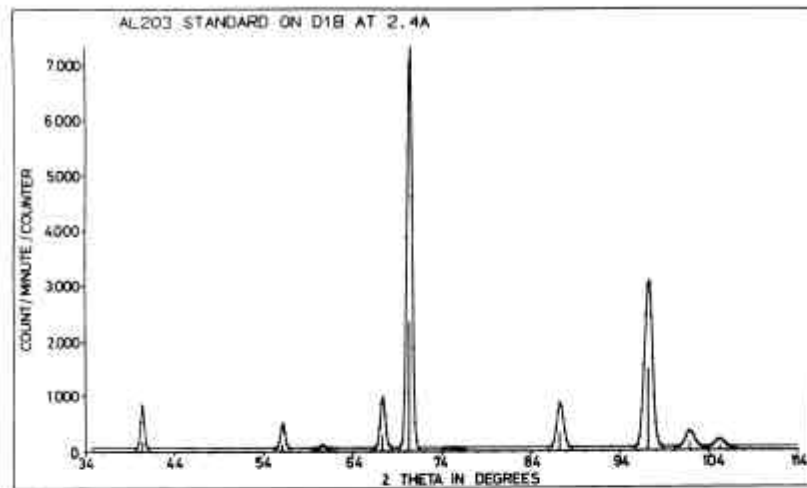
b) Bad compromise



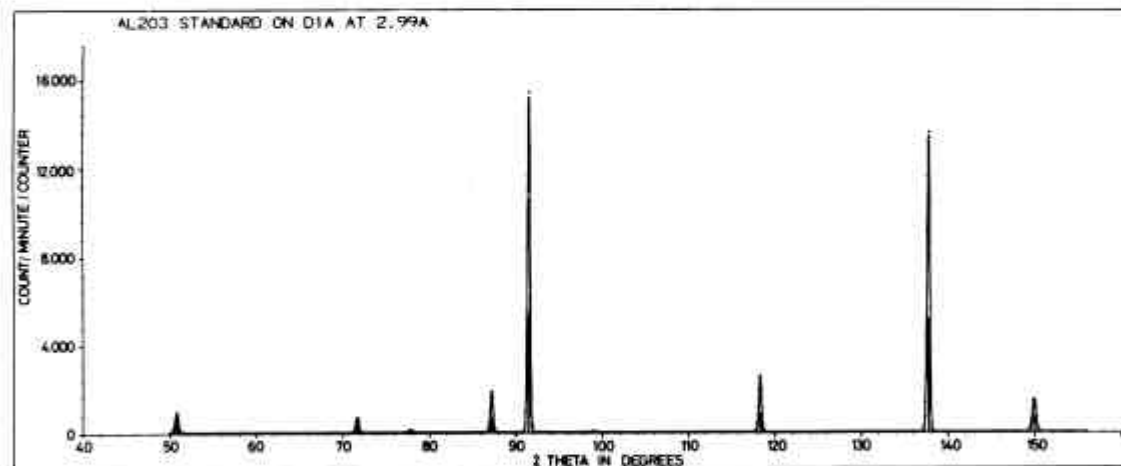
(a)



(b)



(c)



(d)

Fig. 4. (a) Observed and calculated composite profile for the Al_2O_3 standard sample on D1A at $\lambda = 1.384 \text{ \AA}$. The six separate profiles have been averaged in the regions where they overlap (most of the range), so the statistics are equivalent to a single profile six times as intense. (b) Observed and calculated profiles for the same sample on D2 at $\lambda = 1.48 \text{ \AA}$. The intensity per counter is very high, but only one of the four counters could be used at this time because of differences between the collimators. This problem will be overcome when new mylar collimators are fitted as on D1A. (c) Observed and calculated profiles for the standard sample on D1B at $\lambda = 2.4 \text{ \AA}$. All 400 channels are collected simultaneously, so the intensity is effectively 400 times

that shown for the individual counters. (d) Observed and calculated profiles for the same sample on D1A at 2.99 \AA . The resolution at low $\sin \theta/\lambda$ is much improved, and this is useful for magnetic structures, for deciding the symmetry of "pseudo-symmetric" structures, and for help in finding a suitable starting model for profile refinement. The individual peak intensity is almost doubled again in going to $\lambda = 5.7 \text{ \AA}$; the diffraction pattern is not shown for this wavelength, since the dispersion is so great that only the first peak of Al_2O_3 can be seen out to $2\theta = 160^\circ$. Such a long wavelength, with a beryllium filter, could be used to resolve structures with cell dimensions of up to 30 \AA .

High efficiency PSD D1b compared to high resolution D1a



Refinements of Al_2O_3 standard

TABLE I

Structural parameters for Al_2O_3 determined on the new and old D1A, and on D1B and D2. The standard deviation calculated for the cell edge a_0 assumes that the wavelength is known precisely, and does not include any systematic errors, due to sample misplacement for example. The rhombohedral angle, scattering length b_{Al} and structural parameters $u(\text{Al})$ and $u'(0)$ are in surprisingly good agreement for three such very different diffractometers. The Debye-Waller factors $B_{ij} = 8\pi^2 \langle U^2 \rangle_{ij}$ contain systematic errors due to uncertainty in the background subtraction for D2, and because only low order reflexions are available on D1B. The R -factor for D1B is small because there are so few reflexions to fit, and on D2 because the low resolution again means a small amount of data for the number of parameters.

	New D1A	Old D1A	D1B	D2	Other work (X-ray)
a_0	5.13448 (5)	(5)	(60)	(80)	
α	55.270 (1)	55.270 (1)	55.269 (6)	55.268 (6)	55.266 ¹²⁾ 55.277 ¹²⁾ 55.289 ¹³⁾
b_{Al}	0.349 (2)	0.349 (4)	0.345 (16)	0.345 (3)	
b_0	0.580				
$U(\text{Al})$	0.35222 (7)	0.35219(12)	0.35225(36)	0.35261(14)	0.352 ¹⁴⁾
$U'(0)$	0.55635 (8)	0.55621(17)	0.55645(51)	0.55596(23)	0.556 ¹⁴⁾
$B_{11}(\text{Al})$	0.22 (2)	0.19 (5)	0.00 (50)	0.08 (7)	
$B_{12}(\text{Al})$	-0.07 (1)	-0.05 (2)		-0.02 (4)	
$B_{11}(0)$	0.22 (1)	0.34 (3)	-0.10 (45)	0.08 (4)	
$B_{33}(0)$	0.15 (2)	0.22 (3)		0.05 (8)	
$B_{12}(0)$	-0.06 (1)	-0.14 (3)		-0.09 (5)	
$B_{13}(0)$	-0.06 (1)	-0.08 (1)		0.03 (3)	
R_F	0.96	1.35	0.50	0.71	
χ^2	5.68	8.45	5.70	4.48	



Relative Efficiencies of D1a & D1b

TABLE 2

Al_2O_3 standard sample (113) peak intensities per counter, I_{peak} , corrected for the “Lorentz factor” $1/\tan \theta$, together with $\Delta d/d$, the smallest resolvable difference in lattice spacing d . D1A has good resolution $\Delta d/d = \Delta\theta \cot \theta$ because the focussing angle $\theta = 61^\circ$ is large and the collimation $\Delta\theta \lesssim 10'$ is good. With guide tube losses, the intensity per counter is much the same as for an instrument such as PANDA on the medium flux reactor at Harwell, but the effective intensity of D1A is much higher because there are ten counters which can be added. D1B, with 400 counting elements is the most efficient machine, but the best resolution can only be obtained with a sample 1/8th as large. D2 has the highest intensity for single counter applications (e.g., θ - 2θ scans).

	λ (Å)	I_{peak} (c/min)	$I/\tan \theta$	$10^3 \Delta d/d$
D1A	1.38	$9\,500 \times 10$	$26\,700 \times 10$	2
D1B	2.40	$7\,200 \times 400$	$11\,600 \times 400$	8
D2	1.48	95 000	250 000	18
PANDA I	1.48	7 500	19 700	8
Petten	2.57	15 900	24 000	7
BNL	2.41	71 000	114 000	10
Oak Ridge	1.07	11 700	42 400	18

The high resolution D1a multi-detector HRPD and the high efficiency D1b (PSD) position sensitive detector, were also more efficient than others.